Iranian Journal of Mathematical Sciences and Informatics
Vol. 16, No. 2 (2021), pp 125-143
DOI: 10.29252/ijmsi.16.2.125

WENO-Z Schemes with Legendre Basis for non-Linear Degenerate Parabolic Equations

Rooholah Abedian

School of Engineering Science, College of Engineering,
University of Tehran, Iran.

E-mail: rabedian@ut.ac.ir

Abstract. This paper provides a fourth-order scheme for approximating solutions of non-linear degenerate parabolic equations that their solutions may contain discontinuity. In the reconstruction step, a fourth-order weighted essentially non-oscillatory (WENO) reconstruction in Legendre basis, written as a convex combination of interpolants based on different stencils, is constructed. In the one-dimensional case, the new fourth-order reconstruction is based on a four-point stencil. The most important subject is that one of these interpolation polynomials is taken as a quadratic polynomial, and the linear weights of the symmetric and convex combination are set as to get fourth-order accuracy in smooth areas. Following the methodology of the traditional WENO-Z reconstruction, the non-oscillatory weights is calculated by the linear weights. The accuracy, robustness, and high-resolution properties of the new procedure are shown by extensive numerical examples.

Keywords: WENO schemes, Legendre orthogonal polynomials, Multidimensional non-linear degenerate parabolic equations, Porous medium equation.

2020 Mathematics subject classification: 65M06, 35K65.

Received 07 March 2018; Accepted 21 December 2020

1. Introduction

This paper aims at obtaining the numerical solutions of non-linear degenerate parabolic equations of the form

$$u_t = \sum_{j=1}^{d} \frac{\partial^2 b_j(u)}{\partial x_j^2} + S(\mathbf{x}, t, u), \quad \mathbf{x} = (x_1, \cdots, x_d) \in \Omega \subset \mathbb{R}^d, \qquad t \geq 0, \tag{1.1}$$

satisfying the initial function

$$u(\mathbf{x}, 0) = u_0(\mathbf{x}), \qquad \mathbf{x} \in \Omega \subset \mathbb{R}^d, \tag{1.2}$$

and suitable boundary conditions, where d is the space dimension and Ω is an open set. The condition $D_j(u) = b_j'(u) \geq 0;\ j = 1, \cdots, d$ is required to make the equation formally parabolic. The equation degenerates whenever $D_j(u) = 0$ for some $u \in \mathbb{R}$.

For $b_j(u) = u^m,\ m > 1$ and $S(\mathbf{x}, t, u) = 0$, (1.1) is named porous medium equation (PME) [34]. Eqs. (1.1) and (1.2) have at most one weak solution that has compact support in space, if the initial function has compact support (Theorem 5.3 of [34]). Applications of the degenerate parabolic equations can be listed such as: spread of viscous fluids [10], mathematical biology [5], groundwater [4], heat transfer [15], flow of an isentropic gas through a porous medium [34] and other fields.

There are various schemes for obtaining solutions of Eq. (1.1) such as local discontinuous Galerkin finite element method [37], relaxation scheme [8], kinetic scheme [2]. Author's of [25] introduced two different methodology of WENO procedure for obtaining the numerical solutions of non-linear degenerate parabolic equations. Directly approximating to the second derivative term using a conservative flux difference is the first procedure. The second idea which is alike to the approach of the local discontinuous Galerkin (LDG) schemes [9], starts by introducing an auxiliary variable for the first derivative, then uses the WENO procedure to two first derivatives rather than to the second derivative term directly.

In the literature, WENO procedure was introduced to approximate hyperbolic conservation laws. WENO methods are based upon the essentially non-oscillatory (ENO) schemes [16]. The first version of WENO schemes was presented in finite volume fashion for the one-dimensional conservation laws in 1994 by Liu, Osher and Chan [24]. Afterwards, author's of [20] noticed that the ENO stencil selection is sensitive to the round-off perturbation near zeros of the solution and its derivatives. Accordingly, they corrected the ENO reconstruction, and proposed a general framework for sketching arbitrary order accurate finite difference WENO schemes, which are more efficient for multidimensional calculations.

The degenerate parabolic equation (1.1) may have discontinuous solution, possible being of sharp fronts and finite speed of propagation of wave fronts

[34]. The degenerate parabolic equations usually have specifications similar to those of a hyperbolic conservation laws. Accordingly for solving (1.1), it is advisable to distribute numerical methods for solving hyperbolic conservation laws, such as the WENO schemes [25].

WENO reconstructions cannot be used directly to construct a monotone scheme [31] if negative linear weights are present. There are several researches to solve this difficulty: splitting technique [29], regrouping of stencils [19] and reducing the order of accuracy [11]. Without resorting to complex tactics or limiting the generality of a WENO procedure, in this paper, a new approach to remove this difficulty is considered. Using and extending the idea of [23], a fourth-order non-oscillatory finite difference method for solving non-linear degenerate parabolic equations is proposed. The main superiority of this procedure is that the selection of linear weights has no influence on the properties of discretization. Any symmetric election of the constants that their sum is one, defining the linear weights, will enable the desired accuracy.

The new reconstruction is based on defining a suitable quadratic function which is added to linear interpolants in such way as to obtain fourth-order accuracy in smooth areas. In areas with discontinuities or large gradients, the weights are automatically changed so that they switch to a one-sided second-order linear reconstruction.

The structure of this paper is as follows: Section 2 describes by detailing the construction and implementation of the new scheme, for non-linear degenerate parabolic equations. Section 3 gives the results of numerical experiments conducted with proposed scheme in current research. Some remarks are made in Section 4.

2. Non-oscillatory Reconstruction with Legendre Basis to the Second Derivative

This section describes a fourth-order WENO finite difference scheme for multidimensional non-linear degenerate parabolic equation. Using the dimension by dimension approach [31], proposed scheme for multidimensional problems is implemented.

2.1. **General framework.**

Consider the one-dimensional non-linear degenerate parabolic equation

$$u_t = b(u)_{xx} + S(x,t,u), \qquad (x,t) \in \Omega \times (0,\infty), \tag{2.1}$$

$$u(x,0) = u_0(x), \tag{2.2}$$

along with suitable boundary conditions. For simplicity, consider a uniform spatial grid where the cell $I_x = [x - \frac{\Delta x}{2}, x + \frac{\Delta x}{2}]$ has a width Δx. Therefore, x is the mid-cell grid point of I_x, and denote $u(x_j,t)$ and $x_j + i\Delta x$ by $u_j(t)$ and

x_{j+i}, respectively. The following conservative finite difference scheme for Eq. (2.1) is considered.

$$\frac{du_j(t)}{dt} = \frac{\hat{f}_{j+\frac{1}{2}} - \hat{f}_{j-\frac{1}{2}}}{\Delta x^2} + S(x_j, t, u_j(t)), \tag{2.3}$$

where the term

$$\hat{f}_{j+\frac{1}{2}} = f(u_{j-s}, \cdots, u_{j+s+1}), \tag{2.4}$$

is the numerical flux function [25]. The numerical flux $\hat{f}_{j+\frac{1}{2}}$ is chosen so that for all sufficiently smooth u

$$\frac{\hat{f}_{j+\frac{1}{2}} - \hat{f}_{j-\frac{1}{2}}}{\Delta x^2} = (b(u))_{xx}|_{x=x_j} + \mathcal{O}(\Delta x^{(2s+2)}). \tag{2.5}$$

Also, the numerical flux function $\hat{f}_{j+\frac{1}{2}}$ must generate non-oscillatory solutions when the solution contains possible discontinuities [25]. The collection of cells $S = \{I_{j-s}, \cdots, I_{j+s+1}\}$ involving in the numerical flux function is called the stencil for the flux approximation. In this paper, s=1 is considered. Suppose, we can find a function $h(x)$ such that

$$b(u(x)) = \frac{1}{\Delta x^2} \int_{I_x} \int_{I_\eta} h(\xi) d\xi d\eta, \tag{2.6}$$

or equivalent, we can find a differentiable function $v(x)$ such that

$$b(u(x))_x = \frac{1}{\Delta x} \int_{I_x} v'(\eta) d\eta, \ v(x) = \frac{1}{\Delta x} \int_{I_x} h(\eta) d\eta. \tag{2.7}$$

Therefore,

$$b(u(x))_{xx} = \frac{1}{\Delta x} \left(v'(x + \frac{\Delta x}{2}) - v'(x - \frac{\Delta x}{2}) \right), \tag{2.8}$$

$$v'(x) = \frac{1}{\Delta x} \left(h(x + \frac{\Delta x}{2}) - h(x - \frac{\Delta x}{2}) \right) := \frac{g(x)}{\Delta x}, \tag{2.9}$$

then clearly

$$b(u(x))_{xx}|_{x=x_j} = \frac{g(x_{j+\frac{1}{2}}) - g(x_{j-\frac{1}{2}})}{\Delta x^2}. \tag{2.10}$$

2.2. **A fourth-order WENO reconstruction with Legendre basis.** The Legendre orthogonal monic polynomials, shifted for the domain $[0, 1]$, are introduce by

$$\begin{aligned}
L_0(x) &= 1,\\
L_1(x) &= x - \frac{1}{2},\\
L_2(x) &= x^2 - x + \frac{1}{6},\\
L_3(x) &= x^3 - \frac{3}{2}x^2 + \frac{3}{5}x - \frac{1}{20}.
\end{aligned}$$

In the absence of large gradients, a reconstruction with fourth-order accuracy can be obtained if the *optimal* polynomial

$$R_j(x) = p_{\text{opt}}(x),$$

where it is a quadratic polynomial that is chosen. To obtain this *optimal* polynomial, first, a polynomial of degree three on the stencil $S = \{I_{j-1}, \cdots, I_{j+2}\}$, denoted by

$$q(x) = \sum_{i=0}^{3} a_i L_i(\frac{x - x_j}{\Delta x}),$$

is considered to approximate $h(x)$. Next, substituting $q(x)$ into (2.6) and integrating, $b(u(x))$ is computed. Then, using the given point-values of $b(u(x))$ on S, a linear system of four equations in four unknown coefficients is obtained and the coefficients can be obtained explicitly. Finally, Eq. (2.9) determines $p_{\text{opt}}(x)$ completely, namely,

$$p_{\text{opt}}(x) := q(x + \frac{\Delta x}{2}) - q(x - \frac{\Delta x}{2}) = \sum_{i=0}^{2} a_i L_i(\frac{x - x_j}{\Delta x}), \tag{2.11}$$

with

$$\begin{cases} a_0 = \frac{1}{3}b(u_{j-1}) - \frac{1}{2}b(u_j) + \frac{1}{6}b(u_{j+2}), \\ a_1 = \frac{1}{2}b(u_{j-1}) - \frac{1}{2}b(u_j) - \frac{1}{2}b(u_{j+1}) + \frac{1}{2}b(u_{j+2}), \\ a_2 = -\frac{1}{2}b(u_{j-1}) + \frac{3}{2}b(u_j) - \frac{3}{2}b(u_{j+1}) + \frac{1}{2}b(u_{j+2}). \end{cases} \tag{2.12}$$

However, when discontinuities or large gradients occur, this reconstruction would be oscillatory. Accordingly, following the WENO procedure [24, 20, 23, 7] an ENO interpolant is constructed as a convex combination of polynomials that are based on different stencils, i.e.

$$R_j(x) \equiv \sum_i w_i p_i(x), \qquad w_i \geq 0, \ \sum_i w_i = 1, \ i \in \{l, c, r\}, \tag{2.13}$$

where p_l and p_r are linear polynomials based on stencils $S^l = \{I_{j-1}, I_j, I_{j+1}\}$ and $S^r = \{I_j, I_{j+1}, I_{j+2}\}$, respectively, and p_c is a quadratic function. Following a similar argument, these functions can be obtained. For $p_l(x) = a_0 + a_1 L_1(\frac{x-x_j}{\Delta x})$, the coefficients are

$$a_0 = b(u_{j-1}) - b(u_j), \ a_1 = b(u_{j-1}) - 2b(u_j) + b(u_{j+1}). \tag{2.14}$$

Also, for $p_r(x) = a_0 + a_1 L_1(\frac{x-x_j}{\Delta x})$, the coefficients are

$$a_0 = b(u_{j+1}) - b(u_j), \ a_1 = b(u_j) - 2b(u_{j+1}) + b(u_{j+2}). \tag{2.15}$$

Now, the centred function, p_c, should be obtained such that the convex combination (2.13) will be fourth-order accurate in smooth regions. It must, therefore, satisfy

$$p_{\text{opt}}(x) = C_l p_l(x) + C_c p_c(x) + C_r p_r(x), \sum_{i \in \{l,c,r\}} C_i = 1, \tag{2.16}$$

where C_l, C_c and C_r are constants. By a simple calculation it can be observed that any symmetric election of constants C_i in (2.16) enables the desired accuracy. In particular, for the specific choice of $C_l = C_r = \frac{1}{4}$, Eqs. (2.14)–(2.16) yield

$$p_c(x) = 2p_{\rm opt}(x) - \frac{1}{2}(p_l(x) + p_r(x)) = \sum_{i=0}^{2} a_i L_i(\frac{x - x_j}{\Delta x}), \tag{2.17}$$

with

$$\begin{cases} a_0 = \frac{5}{12}b(u_{j-1}) - \frac{3}{4}b(u_j) + \frac{1}{4}b(u_{j+1}) + \frac{1}{12}b(u_{j+2}), \\ a_1 = \frac{1}{2}b(u_{j-1}) - \frac{1}{2}b(u_j) - \frac{1}{2}b(u_{j+1}) + \frac{1}{2}b(u_{j+2}), \\ a_2 = -b(u_{j-1}) + 3b(u_j) - 3b(u_{j+1}) + b(u_{j+2}). \end{cases} \tag{2.18}$$

Also, the reconstruction must be non-oscillatory near discontinuities. Accordingly the linear weights $C_i,\ i \in \{l, c, r\}$ are changed to non-linear weights w_i. Therefore, following [6],

$$w_i = \frac{\alpha_i}{\sum_k \alpha_k},\ \alpha_i = C_i(1 + \frac{\tau}{IS_i + \epsilon}),\ i, k \in \{l, c, r\}, \tag{2.19}$$

where τ is simply considered as

$$\tau = |IS_r - IS_l|^2.$$

The *smoothness indicators*, IS_i, are responsible for discovering large gradients or discontinuities and automatically switch to the stencil that generates the minimum oscillatory reconstruction in such cases. The definition of the smoothness indicator of [25] is used,

$$IS_i = \sum_k \Delta x^{2k-1} \times \int_{I_{x_{j+\frac{1}{2}}}} \left(\frac{d^k}{dx^k} p_i(x)\right)^2 dx. \tag{2.20}$$

A direct computation, based on Eqs. (2.14), (2.15) and (2.17), yields in a compact form as

$$IS_l = a_1^2 = b_{xx}^2 \Delta x^4 + \frac{1}{6} b_{xx} b_{xxxx} \Delta x^6 + \mathcal{O}(\Delta x^8), \tag{2.21}$$

$$IS_c = a_1^2 + \frac{13}{3} a_2^2 = b_{xx}^2 \Delta x^4 + b_{xx} b_{xxx} \Delta x^5 + (\frac{55}{12} b_{xxx}^2 + \frac{2}{3} b_{xx} b_{xxxx}) \Delta x^6 + \mathcal{O}(\Delta x^7), \tag{2.22}$$

$$IS_r = a_1^2 = b_{xx}^2 \Delta x^4 + 2 b_{xx} b_{xxx} \Delta x^5 + (b_{xxx}^2 + \frac{7}{6} b_{xx} b_{xxxx}) \Delta x^6 + \mathcal{O}(\Delta x^7). \tag{2.23}$$

Parameter ϵ is taken to avoid the division by zero in the denominator. furthermore, this parameter has to ensure two requirements [23]:

(i) $\epsilon + \Delta x^4 b_{xx}^4 \gg |IS - \Delta x^4 b_{xx}^4|$ in smooth regions,

(ii) $\epsilon \ll IS$ near discontinuities or large gradients.

These condition ensure the ENO properties of the interpolation in the areas of discontinuities while preserving the optimal properties of convergence when the solution is smooth. This parameter is usually taken equal to 10^{-6}, and it is independent of the solution. Accordingly, in this paper $\epsilon = 10^{-6}$ is chosen.

2.3. **Analysis of the accuracy of the compact WENO scheme.** Evaluating $p_c(x)$ at $x = x_{j+\frac{1}{2}}$, the numerical flux is obtained on the stencil $S = \{I_{j-1}, \cdots, I_{j+2}\}$,

$$p_c(x_{j+\frac{1}{2}}) = \frac{1}{6}b(u_{j-1}) - \frac{3}{2}b(u_j) + \frac{3}{2}b(u_{j+1}) - \frac{1}{6}b(u_{j+2}). \tag{2.24}$$

Thus, from Eq. (2.6),

$$\begin{aligned} p_c(x_{j+\frac{1}{2}}) = &\tfrac{1}{6\Delta x^2}\left(\int_{I_{x_{j-1}}}\int_{I_\eta} h(\xi)d\xi d\eta - \int_{I_{x_{j+2}}}\int_{I_\eta} h(\xi)d\xi d\eta\right) \\ &-\tfrac{3}{2\Delta x^2}\left(\int_{I_{x_j}}\int_{I_\eta} h(\xi)d\xi d\eta - \int_{I_{x_{j+1}}}\int_{I_\eta} h(\xi)d\xi d\eta\right). \end{aligned} \tag{2.25}$$

Now, let the function $h(\xi)$ be smooth. Substituting the Taylor series expansion of $h(\xi)$ at the grid point x_j into Eq. (2.25),

$$p_c(x_{j+\frac{1}{2}}) = \sum_{i=1}^{2} \frac{(\Delta x)^i}{i!}\frac{d^i h(x_j)}{dx^i} + \frac{1}{12}\frac{d^3 h(x_j)}{dx^3}\Delta x^3 + \mathcal{O}(\Delta x^5). \tag{2.26}$$

From Eq. (2.9),

$$\begin{aligned} g(x_{j+\frac{1}{2}}) &= h(x_{j+1}) - h(x_j) \\ &= \textstyle\sum_{i=1}^{2} \frac{(\Delta x)^i}{i!}\frac{d^i h(x_j)}{dx^i} + \frac{1}{6}\frac{d^3 h(x_j)}{dx^3}\Delta x^3 + \mathcal{O}(\Delta x^4). \end{aligned} \tag{2.27}$$

Comparing (2.26) and (2.27), arrives at

$$p_c(x_{j+\frac{1}{2}}) = g(x_{j+\frac{1}{2}}) - \frac{1}{12}\frac{d^3 h(x_j)}{dx^3}\Delta x^3 + \mathcal{O}(\Delta x^4). \tag{2.28}$$

Also, for calculating $p_c(x_{j-\frac{1}{2}})$, each index must be shifted by -1.

$$p_c(x_{j-\frac{1}{2}}) = g(x_{j-\frac{1}{2}}) - \frac{1}{12}\frac{d^3 h(x_j)}{dx^3}\Delta x^3 + \mathcal{O}(\Delta x^4). \tag{2.29}$$

Following a similar argument,

$$p_l(x_{j\pm\frac{1}{2}}) = p_r(x_{j\pm\frac{1}{2}}) = g(x_{j\pm\frac{1}{2}}) + \frac{1}{12}\frac{d^3 h(x_j)}{dx^3}\Delta x^3 + \mathcal{O}(\Delta x^4). \tag{2.30}$$

Combining (2.13) and (2.16) gives

$$R_j(x) = p_{\text{opt}}(x) + \sum_{i\in\{l,c,r\}} (w_i - C_i) \times p_i(x),\ \forall x \in I_j. \tag{2.31}$$

Evaluating Eq. (2.31) at $x = x_{j+\frac{1}{2}}$, the numerical flux is calculated

$$\begin{aligned} \hat{f}_{j+\frac{1}{2}} &= p_{\text{opt}}(x_{j+\frac{1}{2}}) + \textstyle\sum_{i\in\{l,c,r\}}(w_i - C_i) \times p_i(x_{j+\frac{1}{2}}) \\ &= (g(x_{j+\frac{1}{2}}) - \tfrac{1}{90}\tfrac{d^5 h(x_j)}{dx^5}\Delta x^5 + \mathcal{O}(\Delta x^6)) + (\textstyle\sum_i (w_i - C_i) \times p_i(x_{j+\frac{1}{2}})), \end{aligned} \tag{2.32}$$

where the second parenthesis must be at least $\mathcal{O}(\Delta x^5)$ in smooth areas, in order to warranty the approximation to the second order derivative to be fourth-order accurate. Expanding the second parenthesis and substituting Eqs. (2.28) and (2.30), give

$$\begin{aligned}&\sum_i (w_i - C_i) \times p_i(x_{j+\frac{1}{2}}) = \\ &(w_l - w_c + w_r)\tfrac{1}{12}\tfrac{d^3 h(x_j)}{dx^3}\Delta x^3 + \sum_i (w_i - C_i)\Delta x^4,\ i \in \{l, c, r\},\end{aligned} \tag{2.33}$$

because of $C_l = C_r = \frac{1}{2}C_c$ and $\sum_i C_i = \sum_i w_i = 1$. Therefore, the necessary and sufficient conditions are

$$\begin{cases} w_l - w_c + w_r \leq \mathcal{O}(\Delta x^3), \\ \\ w_i - C_i \leq \mathcal{O}(\Delta x^2),\ i \in \{l, c, r\}. \end{cases} \tag{2.34}$$

From Eqs. (2.21) and (2.23), it is easy to see

$$IS_r - IS_l = 2b_{xx}b_{xxx}\Delta x^5 + (b_{xxx}^2 + b_{xx}b_{xxxx})\Delta x^6 + \mathcal{O}(\Delta x^7). \tag{2.35}$$

Hence,

$$\tau = |IS_r - IS_l|^2 = \begin{cases} \mathcal{O}(\Delta x^{10}),\ b_{xx}|_{x_i} \neq 0, b_{xxx}|_{x_i} \neq 0, \\ \\ \mathcal{O}(\Delta x^{12}),\ o.w. \end{cases} \tag{2.36}$$

In smooth regions and on condition that $\epsilon << IS_i$ where $i \in \{l, c, r\}$, it derives

$$\frac{\tau}{\epsilon + IS_i} = \mathcal{O}(\Delta x^6),$$

hence $\alpha_i = C_i + \mathcal{O}(\Delta x^6)$. By definition w_i in Eq. (2.19), it concludes $w_i = C_i + \mathcal{O}(\Delta x^6)$ and $w_l - w_c + w_r = C_l - C_c + C_r + \mathcal{O}(\Delta x^6) = \mathcal{O}(\Delta x^6)$ because of $C_l = C_r = \frac{1}{2}C_c$. Therefore, the condition (2.34) is satisfied and the new scheme has fourth-order accuracy for smooth solutions and is non-oscillatory near discontinuities.

Then, the final form of the new scheme for non-linear degenerate parabolic equations is given by

$$\frac{du_j(t)}{dt} = \frac{\hat{f}_{j+\frac{1}{2}} - \hat{f}_{j-\frac{1}{2}}}{\Delta x^2} + S(x_j, t, u_j(t)) = F(u_j(t)), \tag{2.37}$$

with the approximation flux

$$\hat{f}_{j+\frac{1}{2}} = \sum_{i \in \{l,c,r\}} w_i p_i(x_{j+\frac{1}{2}}). \tag{2.38}$$

Remark 1. As already noted in [25], when applying the standard WENO idea, as is done in Liu et al. [25], in some cases the linear weights don't exist for

$$\hat{f}_{j+\frac{1}{2}} = \sum_m C_m p_m(x_{j+\frac{1}{2}})$$

to hold, and when they do exist, at least one of them is negative. For example, Liu et al. must have

$$C_0 = -\frac{2}{15}, \qquad C_1 = \frac{19}{15}, \qquad C_2 = -\frac{2}{15}$$

to obtain the sixth-order accuracy. Therefore, they split the linear weights into two parts, positive and negative, by defining

$$\tilde{\gamma}_m^+ = \frac{1}{2}(C_m + \theta|C_m|), \qquad \tilde{\gamma}_m^- = \tilde{\gamma}_m^+ - C_m,\ m = 0, 1, 2,$$

where $\theta = 3$. By scaling $\sigma^\pm = \sum_{m=0}^{2} \tilde{\gamma}_m^\pm$, the linear weights of the two parts are obtained by $\gamma_m^\pm = \frac{\tilde{\gamma}_m^\pm}{\sigma^\pm}$. It is easy to check that

$$\sum_{m=0}^{2} \gamma_m^\pm = 1, \qquad C_m = \sigma^+\gamma_m^+ - \sigma^-\gamma_m^-.$$

As we can see from the above, with our strategy, one can overcome these difficulties.

Remark 2. consider d-cube $\Omega = [a_1, b_1] \times \cdots \times [a_d, b_d]$ domain covered by cells $[x^1_{j_1-\frac{1}{2}}, x^1_{j_1+\frac{1}{2}}] \times \cdots \times [x^d_{j_1-\frac{1}{2}}, x^d_{j_1+\frac{1}{2}}]$ where $j_i = 0, \cdots, N_i,\ i = 1, \cdots, d$, the centres of the cells are $x^i = \frac{1}{2}(x^i_{j_i+\frac{1}{2}} + x^i_{j_i-\frac{1}{2}})$, and we define $\Delta x^i = x^i_{j_i+\frac{1}{2}} - x^i_{j_i-\frac{1}{2}}$. Therefore, direct conservative approximation to the spatial derivative for Eq. (1.1) gives

$$\frac{du_{\mathbf{j}}(t)}{dt} = \sum_{i=1}^{d} \frac{\hat{f}^i_{j+\frac{1}{2}} - \hat{f}^i_{j-\frac{1}{2}}}{(\Delta x^i)^2} + S(\mathbf{x_j}, t, u_{\mathbf{j}}(t)), \tag{2.39}$$

where $u_{\mathbf{j}}(t)$ is the numerical approximation to the point value $u(\mathbf{x_j}, t)$ in which $\mathbf{x_j} = (x^1_{j_1}, \cdots, x^d_{j_d})$ and $\mathbf{j} = (j_1, \cdots, j_d)$. The numerical flux $\hat{f}^i_{j+\frac{1}{2}}$ is obtained by the one-dimensional compact WENO approximation procedure, describing in previous subsections. Also, in multidimensional problems, the nonlinear weights and the smoothness indicators are calculated by a dimension-by-dimension fashion.

3. Computational Results

3.1. **Time evolution method.** There are several time evolution schemes for the semi-discrete Eq. (2.37). The most commonly used are the strong-stability preserving Runge-Kutta (SSPRK) schemes [32, 33], and further developed in [14, 13]. Also, a class of total variation diminishing multi-step schemes is proposed in [30], but these schemes need different and sometimes costlier treatment for their negative coefficients. In this work, the numerical solution is advanced in time by means of the linear multistep total variation bounded (TVB_0) scheme, proposed by Ruuth and Hundsdorfer in [28]. We would like to emphasize that this scheme does not need additional treatments for negative coefficients and that it possesses relaxed monotonicity or boundedness properties with optimal step size conditions, that is, it improves the step size restriction of the Courant-Friedrichs-Lewy (CFL) number. The TVB_0 schemes allow higher effective CFL numbers than SSPRK schemes. However, this is done at the expense of a higher storage. Authors of [28] demonstrated that their scheme avoided the undershoots generated by SSPRK or other multi-step methods for large time steps. Also, they claimed that their new scheme is more efficient in terms of CPU time compared to SSPRK. Our semi-discrete finite difference mapped WENO scheme is advanced in time by means of the fourth-order five-step high-order linear multi-step scheme, $\mathrm{TVB}_0(5,4)$ which is given by

$$\begin{aligned} u_j^{n+1} &= 3.089334754787739u_j^n + 1.629978886421390\Delta t F_j^n \\ &-3.997727108450201u_j^{n-1} - 3.839438825282836\Delta t F_j^{n-1} \\ &+2.799704082644115u_j^{n-2} + 3.698752623531085\Delta t F_j^{n-2} \\ &-1.069321620028803u_j^{n-3} - 1.688757722449064\Delta t F_j^{n-3} \\ &+0.178009891047150u_j^{n-4} + 0.305220798719644\Delta t F_j^{n-4}. \end{aligned} \tag{3.1}$$

The $\mathrm{TVB}_0(5,4)$ scheme gives solutions without any visible or excessive smearing up to the CFL (Courant-Friedrichs-Lewy) number $c = 0.450202335599730$. In the current work, we obtain the first steps of the linear multi-step scheme using the third-order total variation diminishing (TVD) Runge-Kutta scheme [32], which is given by

$$\begin{aligned} u_j^{(1)} &= u_j^n + \Delta t F(u_j^n), \\ u_j^{(2)} &= \tfrac{3}{4}u_j^n + \tfrac{1}{4}u_j^{(1)} + \tfrac{1}{4}\Delta t F(u_j^{(1)}), \\ u_j^{n+1} &= \tfrac{1}{3}u_j^n + \tfrac{2}{3}u_j^{(2)} + \tfrac{2}{3}\Delta t F(u_j^{(2)}). \end{aligned} \tag{3.2}$$

3.2. **Multidimensional problems.** This section will present some numerical tests to acknowledge the accuracy, robustness, and high-resolution features of the new scheme. Example 1 is a 3D heat equation with a known exact solution and is applied for studying the accuracy and order of convergence [25]. Example 2 is the 2D porous medium equation [25]. In Example 3, a non-linear problem, suggested as test for multi-dimensional non-linear convection-diffusion problems [21, 1] is considered. Next, in Example 4, a scalar 2D reaction-diffusion equation [5] is solved. Finally, Example 5 taken from [22, 18], is presented to cover the case strongly degenerate parabolic equation. The CFL number $c = 0.4$ is chosen which is within the stability range of the $\mathrm{TVB}_0(5,4)$ ($c = 0.450202335599730$) time method [28]. Then, the time step is calculated

TABLE 1. Errors for Example 1 at $T = 2$. ($A(-e) := A \times 10^{-e}$)

N	L_∞ error	L_∞ order	L_1 error	L_1 order
10	0.246(-1)	-	0.876(-2)	-
20	0.163(-2)	3.915	0.509(-3)	4.105
40	0.875(-4)	4.219	0.300(-4)	4.085
80	0.484(-5)	4.176	0.183(-5)	4.035
160	0.280(-6)	4.111	0.114(-6)	4.004

by

$$\max_u |b'(u)| \frac{\Delta t}{(\Delta x)^2} = 0.4.$$

Let $u(x_j, t^n)$ and w_j^n be the exact solution and the reconstructed solution respectively at (x_j, t^n). Then the norms of the error are given by :

$$\begin{aligned} L_1 - \text{error} \qquad & ||u-w||_1 = \sum_{j=1}^{N} |u(x_j,t^n) - w_j^n| \Delta x, \\ L_\infty - \text{error} \qquad & ||u-w||_\infty = \max_{1 \leqslant j \leqslant N} |u(x_j,t^n) - w_j^n|. \end{aligned}$$

Remark. It should be noted that L_1 norm examines the sum of errors generated by a numerical scheme, while L_∞ norm examines the numerical method's ability to investigate the shock or jump discontinuity in solution. The higher order of convergence, the faster the numerical method achieves the desired accuracy. Also,

$$L_p - \text{order} := \frac{\log(L_p - \text{error with N}) - \log(L_p - \text{error with 2N})}{\log 2}.$$

In the following CWENO4 is applied to denote the new proposed method in the current paper.

Example 1. For $\mathbf{x} = (x, y, z),\ b_j(u) = u; j = 1, 2, 3$ and $S(\mathbf{x}, t, u) \equiv 0$, consider the 3D linear initial-value problem with periodic boundary conditions in all directions [25],

$$\begin{cases} u_t = u_{xx} + u_{yy} + u_{zz},\ \mathbf{x} \in \Omega = (-\pi, \pi)^3,\ t > 0, \\ u(x, y, z, 0) = \sin(x)\sin(y)\sin(z). \end{cases}$$

The exact solution of this problem is $u(x, y, z, t) = \exp(-t)\sin(x)\sin(y)\sin(z)$. In Table 1, the respective errors and orders of convergence by CWENO4 are presented. The results verify the fourth-order accuracy both in the L_∞ and in the L_1 norms.

Example 2. Consider the porous medium equation (PME) as [25]

$$u_t = \Delta(u^m),\ m > 1, \tag{3.3}$$

where $u = u(\mathbf{x}, t),\ \mathbf{x} \in \Omega \subset \mathbb{R}^d$. This equation describes various diffusion processes, such as the flow of an isentropic gas through a porous medium where

TABLE 2. Errors for Example 2 at $T=2$. ($A(-e) := A \times 10^{-e}$)

	$m=2$		$m=4$	
N=cells	L_∞ error	L_1 error	L_∞ error	L_1 error
50	0.015(-1)	0.433(-1)	0.121(-1)	0.253
100	0.011(-1)	0.176(-1)	0.088(-1)	0.644(-1)
200	0.008(-1)	0.040(-1)	0.075(-1)	0.261(-1)
400	0.004(-1)	0.008(-1)	0.061(-1)	0.099(-1)
	$m=6$		$m=8$	
50	0.218(-1)	0.358	0.341(-1)	0.589
100	0.238(-1)	0.138	0.251(-1)	0.205
200	0.182(-1)	0.730(-1)	0.217(-1)	0.759(-1)
400	0.138(-1)	0.253(-1)	0.222(-1)	0.373(-1)

u is the density of the gas required to be non-negative and u^{m-1} is the pressure of the gas. The PME equation degenerates at points where $u=0$, resulting in the phenomenon of finite speed of propagation and sharp fronts. We would like to emphasize that the classical solutions to the PME may not exist in general, even if the initial condition is smooth. The closed analytical form which is a weak solution for PME, is obtained by Zel'dovich and Kompaneets [36] and Barenblatt [3] in years 1950 and 1952 respectively. The solution of [3] has the following explicit form

$$u(\mathbf{x},t) = t^{-\alpha}\left[\left(1-k|\mathbf{x}|^2 t^{-\frac{2\alpha}{d}}\right)_+\right]^{\frac{1}{m-1}}, \tag{3.4}$$

where $\alpha = \frac{d}{(m-1)d+2}$, $k = \frac{\alpha(m-1)}{2md}$ and $u_+ = \max(u,0)$. Now, we put $d = 2$, therefore, Barenblatt solution has no derivative at the points of the circle $x^2+y^2 = \sqrt{\frac{4m}{\alpha(m-1)}}t^\alpha$ where $\alpha = \frac{1}{m}$. CWENO4 scheme is applied to solve the PME (3.3) for $m=2,4,6$ and $m=8$, where $\Omega = [-10,10]^2$. The initial condition is taken as the Barenblatt solution (3.4) at $t=1$, and the boundary condition is chosen to be $u=0$ on $\partial\Omega$ for $t>1$. Table 2 indicates the magnitude of errors obtained with CWENO4 scheme for different mesh sizes. Fig. 1 shows the results of CWENO4 scheme at the Final time $T=3$, with the computational domain Ω divided into 120 uniform cells. As can be seen, the CWENO4 scheme prevents the appearance of spurious solutions close to the circles. The contour plots of absolute difference between approximated solution and Barenblatt solution with $m=2,4$ are shown in Fig. 1 top right and bottom right, respectively. As can be seen, the CWENO4 scheme is sufficiently accurate in the smooth regions, while on the non-smooth regions absolute difference with analytical form solution of Barenblatt is of order 10^{-3} and 10^{-2} for $m=2$ and $m=4$, respectively.

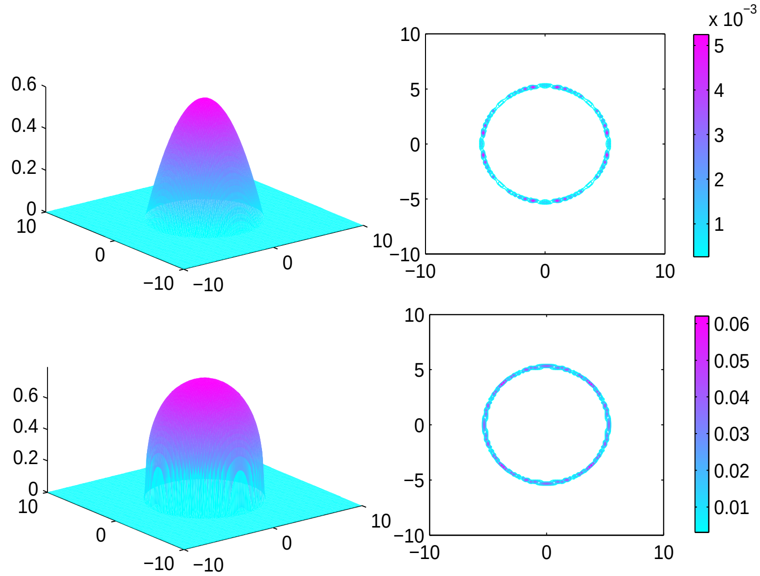

FIGURE 1. Example 2 (two-dimensional porous medium equation). Top left: PME with $m = 2$ and $N = 120$, Top right: 30 contour lines of $|u_{\text{Barenblatt}} - u|$ with $m = 2$, Bottom left: PME with $m = 4$ and $N = 120$, Bottom right: 30 contour lines of $|u_{\text{Barenblatt}} - u|$ with $m = 4$.

Example 3. In this example, we focus on the Buckley-Leverett-type problem [21, 1]

$$u_t + f(u)_x + g(u)_y = \epsilon(u_{xx} + u_{yy}) \tag{3.5}$$

with $\epsilon = 0.1$, the flux function of the form

$$g(u) = \frac{u^2}{u^2 + (1-u)^2},$$

$$f(u) = g(u)(1 - 5(1-u)^2).$$

The initial function for this example is

$$u(x, y, 0) = \begin{cases} 1, & (x - 0.25)^2 + (y - 0.25)^2 < 5, \\ \\ 0, & o.w. \end{cases}$$

This example includes gravitational effects in the x-direction. The numerical results are shown at $T = 0.5$ and 1.0 in Fig. 2 with the computational domain $[-3, 3]^2$ divided into 40×40 uniform cells. The results compare well with those reported in [1]. In Table 3, the respective errors and convergence rates

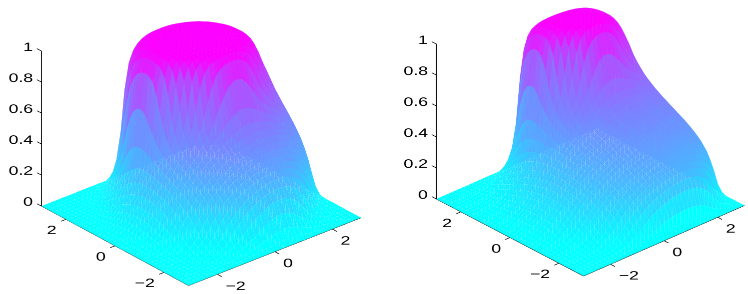

FIGURE 2. Example 3 (two-dimensional Buckley-Leverett-type equation). Left: numerical solution at $T = 0.5$ with $N = 40$, Right: numerical solution at $T = 1.0$ with $N = 40$.

TABLE 3. Errors for Example 3 at $T = 0.5$. ($A(-e) := A \times 10^{-e}$)

N	L_∞ error	L_∞ order	L_1 error	L_1 order
40	0.998(-3)	-	0.137(-2)	-
80	0.728(-4)	3.777	0.973(-4)	3.816
160	0.450(-5)	3.865	0.691(-5)	3.815
320	0.355(-6)	3.813	0.470(-6)	3.880

by CWENO4 are given. The numerical solutions compared with a "reference solution", obtained by WENO6 [25] with $N = 400$.

Example 4. Now, the following initial-boundary-value problem for a scalar reaction-diffusion equation [5] is considered,

$$u_t = \Delta b(u) + S(x, y, t, u), \tag{3.6}$$

$$u(x, y, 0) = 0.5(1 + \sin(1.1(x - \cos(0.7y)))) \cos(0.5(y - \sin(1.3x))), \tag{3.7}$$

$$\nabla b(u) \cdot \mathbf{n} = 0 \text{ on } \partial\Omega \times [0, T]. \tag{3.8}$$

Usually this problem is considered as prototype degenerate reaction-diffusion model. The zero-flux boundary condition (3.8) is considered to mention that the reaction-diffusion domain is isolated from the external surroundings. For $S(x, y, t, u) = S(u)$, Eq. (3.6) appears in an ecological setting [26]. Here, u explains the population density of a species, and $S(u)$ is its dynamics, where it is supposed that $S(0) = 0$ and $S'(0) \neq 0$. For example, $S(u) = u(1 - u) - u^2/(1 + u^2)$ corresponds to the population dynamics of the spruce band-worm [26], and models the growth of the population by a logistic expression and the rate of mortality due to predation by other animals. Authors of [5] corrected this expression by a radial spatial factor, and applied

$$S(x,y,t,u) = 10(\exp(-5r)u(1-u) + (\exp(-5r)-1)\frac{u^2}{1+u^2}), \tag{3.9}$$
$$r = \sqrt{(x-0.5)^2 + (y-0.5)^2},$$

which means that the birth of individuals is concentrated near the centre $(0.5, 0.5)$, and mortality increases with increasing distance from the centre. Most standard spatial models of population dynamics simply assume that $b(u) = Du$, where the constant diffusion coefficient $D > 0$ measures the dispersal efficiency of the species under consideration. In this example, the strongly degenerate diffusion coefficient is used [35, 5]

$$b(u) = \begin{cases} 0, & u \le \frac{1}{2}, \\ u - \frac{1}{2}, & o.w. \end{cases}$$

The difficulty in the well-posedness analysis of the problem (3.6) lies in the boundary condition (3.8) when b is strongly degenerate. It is actually hard to present a accurate formulation of the zero-flux boundary conditions. Fig. 3 demonstrates the numerical approximation with 80×80 uniform cells at different time levels which the outcomes compare well with those reported in [5].

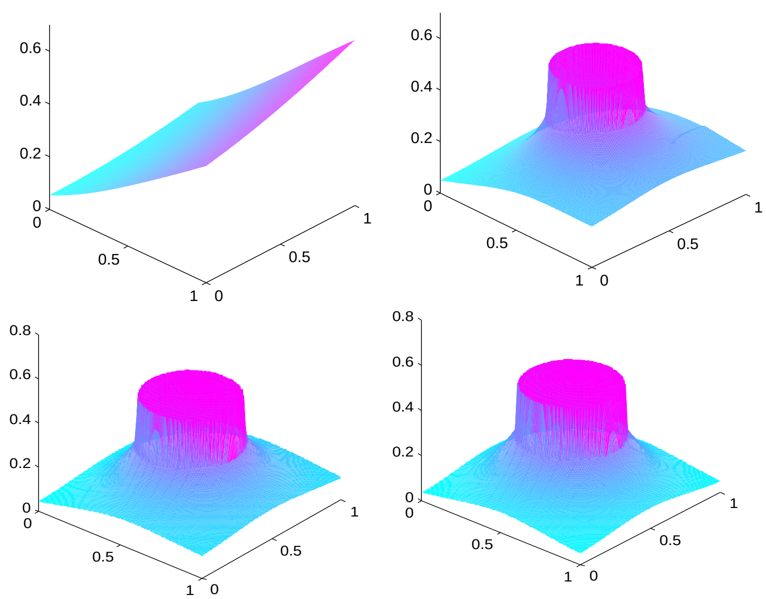

FIGURE 3. Example 4 (single-species reaction-diffusion model). From top left to bottom right, the numerical solution at times $T = 0.0,\ 0.5,\ 1.0,\ 3.0$.

TABLE 4. Errors for example 5 at $T = 0.5$. ($A(-e) := A \times 10^{-e}$)

N	L_∞ error	L_∞ order	L_1 error	L_1 order
40	0.250(-1)	2.491	0.346(-1)	2.279
80	0.400(-2)	2.643	0.500(-2)	2.790
160	0.480(-3)	3.058	0.634(-3)	2.979
320	0.567(-4)	3.082	0.794(-4)	2.997

Example 5. Finally, a strongly degenerate parabolic equation is considered for solving. Consider the Burgers-like equation

$$u_t + (u^2)_x + (u^2)_y = \epsilon(\nu(u)u_x)_x + \epsilon(\nu(u)u_y)_y.$$

We put $\epsilon = 0.1$ and

$$\nu(u) = \begin{cases} 0, & |u| \le 0.25, \\ \\ 1, & |u| > 0.25. \end{cases}$$

zero boundary conditions are assumed in all directions. The initial function is equal to -1 and 1 inside two circles of radius 0.4 centred at $(0.5, 0.5)$ and $(-0.5, -0.5)$ respectively, and zero elsewhere inside the square $[-1.5, 1.5]^2$. With different mesh sizes, the L_∞ and L_1 errors of CWENO4 scheme are presented in Table 4. The numerical results obtained by CWENO4 scheme with 80×80 uniform cells are presented in Fig. 4. The results compare well with those reported in [22, 25]. The "reference solution" was generated by WENO6 [25] scheme with $N = 400$.

4. Conclusion

When using the original WENO idea, as Liu et al. did in [25], in some cases the ideal weights don't exist, and when they do exist, at least one of them is negative. In this research, a new *compact* finite difference WENO scheme was proposed to solve these problems. Our strategy consists in applying the Central WENO procedure of Levy et al. [23], then the new technique results from a convex combination of three functions. Combined with a linear multi-step total variation bounded method for the time-integration, it observed that this algorithm created a fourth-order method in smooth regions and remains essentially non-oscillatory near discontinuities. Computational results showed that the new scheme can generate fourth-order accuracy in smooth regions and prevents the appearance of spurious solutions close to discontinuities.

Acknowledgement

The author is very thankful to the reviewers for carefully reading the paper, their comments and suggestions have improved the quality of the paper.

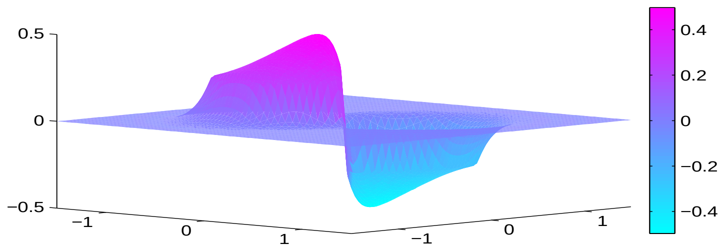

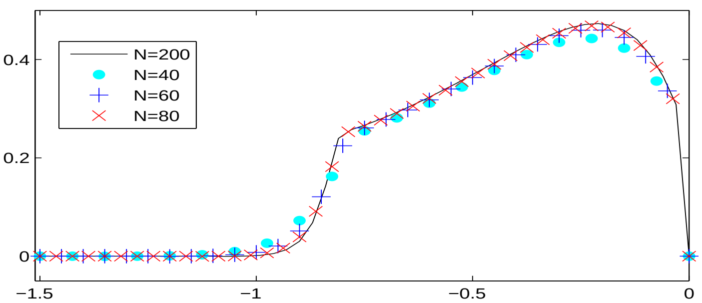

FIGURE 4. Example 5 (two-dimensional strongly degenerate parabolic problem). Top: numerical solution at $T = 0.5$ with $N = 80$, Bottom: one-dimensional cut along the y axis with different mesh sizes.

References

1. C. D. Acosta and R. Bürger, Difference schemes stabilized by discrete mollification for degenerate parabolic equations in two space dimensions, *IMA J. Numer. Anal.*, **32**, (2012), 1509–1540.
2. D. Aregba-Driollet, R. Natalini, S. Tang, Explicit diffusive kinetic schemes for nonlinear degenerate parabolic systems, *Math. Comput.*, **73**, (2004), 63–94.
3. G. I. Barenblatt, On some unsteady motions of a liquid or a gas in a porous medium, *Prikl. Mat. Mekh.*, **16**, (1952), 67–78, in Russian.
4. G. I. Barenblatt, M. Bertsch, A. E. Chertock, V. M. Prostokishin, Self-similar intermediate asymptotics for a degenerate parabolic filtration-absorption equation, *Proc. Natl. Acad. Sci. U. S. A.*, **97**, (2000), 9844–9848.
5. M. Bendahmane, R. Burger, R. Ruiz-Baier, K. Schneider, Adaptive multiresolution schemes with local time stepping for two-dimensional degenerate reaction-diffusion systems, *Appl. Numer. Math*, **59**, (2009), 1668–1692.
6. R. Borges, M. Carmona, B. Costa, W. S. Don, An improved weighted essentially non-oscillatory scheme for hyperbolic conservation laws, *J. Comput. Phys.*, **227**, (2008), 3191–3211.
7. G. Capdeville, A central WENO scheme for solving hyperbolic conservation laws on non-uniform meshes, *J. Comput. Phys.*, **227**, (2008), 2977–3014.
8. F. Cavalli, G. Naldi, G. Puppo, M. Semplice, High order relaxation schemes for nonlinear degenerate diffusion problems, *SIAM J. Numer. Anal.*, **45**, (2007), 2098–2119.

9. B. Cockburn, C.-W. Shu, The local discontinuous Galerkin method for time-dependent convection-diffusion systems, *SIAM J. Numer. Anal.*, **35**, (1998), 2440–2463.
10. B. Davidovitch, E. Moro, A. H. Stone, Spreading of viscous fluid drops on a solid substrate assisted by thermal fluctuations, *Phys. Rev. Lett.*, **95**, (2005), 244–505.
11. M. Dumbser and M. Käser, Arbitrary high order non-oscillatory finite volume schemes on unstructured meshes for linear hyperbolic systems, *J. Comput. Phys.*, **221**, (2007), 693–723.
12. R. Fedkiw, B. Merriman, and S. Osher, *Simplified upwind discretization of systems of hyperbolic conservation laws containing advection equations*, J. Comput. Phys. **157** (2000), 302–326.
13. S. Gottlieb, C.-W.Shu, and E. Tadmor, *Strong stability-preserving high-order time discretization methods*, SIAM Rev. **43** (2001), 89–112.
14. S. Gottlieb and C.-W. Shu, *Total variation diminishing Runge-Kutta schemes*, Math. Comp. **67** (1998), 73–85.
15. C. Harley, *Asymptotic and dynamical analyses of heat transfer through a rectangular longitudinal fin*, J. Appl. Math. **2013** (2013), 1–8.
16. A. Harten, B. Engquist, S. Osher, and S. Chakravarthy, *Uniformly high-order essentially non-oscillatory schemes, III*, J. Comput. Phys. **71** (1987), 231–303.
17. A. K. Henrick, T. D. Aslam, and J. M. Powers, *Mapped weighted essentially non-oscillatory schemes: Achieving optimal order near critical points*, J. Comput. Phys. **207** (2005), 542–567.
18. H. Holden, K. H. Karlsen, and K.-A. Lie, *Operator splitting methods for degenerate convection-diffusion equations II: Numerical examples with emphasis on reservoir simulation and sedimentation*, Comput. Geosci. **4** (2000), 287–322.
19. C. Hu and C.-W. Shu, *Weighted essentially non-oscillatory schemes on triangular meshes*, J. Comput. Phys. **150** (1999), 97–127.
20. G. S. Jiang and C.-W. Shu, *Efficient implementation of weighted ENO schemes*, J. Comput. Phys. **126** (1996), 202–228.
21. K. H. Karlsen and N. H. Risebro, *An operator splitting method for nonlinear convection-diffusion equations*, Numer. Math. **77** (1997), 365–382.
22. A. Kurganov and E. Tadmor, *New high-resolution central schemes for nonlinear conservation laws and convection-diffusion equations*, J. Comput. Phys. **160** (2000), 241–282.
23. D. Levy, G. Pupo, and G. Russo, *Compact central WENO schemes for multidimensional conservation laws*, SIAM J. Sci. Comput. **22** (2000), 656–672.
24. X.-D. Liu, S. Osher, and T. Chan, *Weighted essentially non-oscillatory schemes*, J. Comput. Phys. **115** (1994), 200–212.
25. Y. Liu, C.-W. Shu, and M. Zhang, *High order finite difference WENO schemes for nonlinear degenerate parabolic equations*, SIAM J. Sci. Comput. **33** (2011), 939–965.
26. J. D. Murray, *Mathematical biology II: Spatial models and biomedical applications*, Springer-Verlag, New York, 2003.
27. A. A. I. Peer, M. Z. Dauhoo, and M. Bhuruth, *A method for improving the performance of the WENO5 scheme near discontinuities*, Appl. Math. Lett. **22** (2009), 1730–1733.
28. S. J. Ruuth and W. Hundsdorfer, *High-order linear multistep methods with general monotonicity and boundedness properties*, J. Comput. Phys. **209** (2005), 226–248.
29. J. Shi, C. Hu, and C.-W. Shu, *A technique of treating negative weights in WENO schemes*, J. Comput. Phys. **175** (2002), 108–127.
30. C.-W. Shu, *Total-variation-diminishing time discretizations*, SIAM J. Sci. Stat. Comp. **9** (1988), 1073–1084.

31. C.-W. Shu, *Essentially non-oscillatory and weighted essentially non-oscillatory schemes for hyperbolic conservation laws*, (1997), in: Quarteroni(Ed.), Lecture Notes in Mathematics, Springer, Berlin.
32. C.-W. Shu and S. Osher, *Efficient implementation of essentially non-oscillatory shock-capturing schemes*, J. Comput. Phys. **77** (1988), 439–471.
33. C.-W. Shu and S. Osher, *Efficient implementation of essentially non-oscillatory shock-capturing schemes II*, J. Comput. Phys. **83** (1989), 32–78.
34. J. L. Vàzquez, *The Porous Medium Equation Mathematical Theory*, Oxford University Press Inc, New York, 2007.
35. T. P. Witelski, *Segregation and mixing in degenerate diffusion in population dynamics*, J. Math. Biol. **35** (1997), 695–712.
36. Ya. B. Zeldovich and A. S. Kompaneets, *Towards a theory of heat conduction with thermal conductivity depending on the temperature*, (1950), 61–72, in: Collection of Papers Dedicated to 70th Anniversary of A. F. Ioffe. Izd. Akad. Nauk SSSR, Moscow.
37. Q. Zhang and Z. Wu, *Numerical simulation for porous medium equation by local discontinuous Galerkin finite element method*, J. Sci. Comput. **38** (2009), 127–148.